SCIENTIFIC COMMITTEE
TWENTY-SECOND REGULAR SESSION
11-19 August 2026
Apia, Samoa (Hybrid)

PRELIMINARY REPORT OF "PACIFIC TUNA AND ECOSYSTEM RESEARCH CRUISE PROJECT" IN 2025

WCPFC-SC22-2026-EB-IP13
20 July 2026

Submitted by

Tawa A., Ishihara T., Yamaguchi T., Nagatomo Y., Okazaki M., Ambe D., Hidaka K., Kiyofuji H. [1], Allain V., Vourey E., Barbin L., Magnier P., Portal A., Wirotaroeno L., Pilling G.[2] Ata C., Kafo W.[3]

[1] Japan Fisheries Research and Education Agency, FRA
[2] The Pacific Community, SPC
[3] Solomon Island National University

Preliminary report of “Pacific Tuna and Ecosystem Research Cruise Project” in 2025

Tawa A., Ishihara T., Yamaguchi T., Nagatomo Y., Okazaki M., Ambe D., Hidaka K., Kiyofuji H. (Japan Fisheries Research and Education Agency, FRA)
Allain V., Vourey E., Barbin L., Magnier P., Portal A., Wirotaroeno L., Pilling G. (The Pacific Community, SPC)
Ata C., Kafo W. (Solomon Island National University)

Summary:
This document presents preliminary results from the second year of a new project initiated in 2024, aimed at elucidating the relationship between the early life ecology of tropical tuna and oceanographic conditions in the tropical-subtropical region. The survey, conducted in 2025 using the R/V Kaiyo-Maru in the central and western Pacific Ocean, consisted of two main legs. The first leg (Leg 1) from Harumi in Tokyo to Honiara in Solomon Islands during 27 August and 28 September. It was set to survey an area spanning 170°E–170°W and 0°–5°N. The second leg (Leg 2) from Honiara to Saipan from 2 to 20 October. It surveyed a north-south line on the 150–160°E and 0–15°N. The oceanographic conditions along the Leg 1 transect exhibited the typical characteristics of an equatorial divergence region, except at northwestern stations where potential warm pool conditions were observed. On the other hand, there was a transition from an equatorial divergence region to subtropical gyre along the south-north Leg 2 transect. A total of 1161 tuna larvae were collected by ring net, bongo net and MOC-MOHT. A further 87 tuna juveniles were collected using a midwater trawl at different depths. Preliminarily result from morphological observations and DNA analysis indicate that their tuna larvae and juveniles include *Thunnus albacares*, *Thunnus obesus*, *Thunnus alalunga*, *Katsuwonus pelamis* and *Auxis thazard*. In addition, a stratified collection was conducted using a NORPAC net and a VMPS to clarify the zooplankton that could be the food of tuna larvae. The vertical distribution and densities of zooplankton and micronekton were measured acoustically using WBAT. More detailed analyses of the collected samples are currently in progress, and together with the results from 2024, are expected to advance our understanding of the early life ecology of tropical tuna in this region. This project is also scheduled to be conducted in a different survey area in 2026.

Keywords: Tuna and tuna like fishes・Larval survey・International collaborative research・Pacific Ocean・Climate changes

Introduction

The research project, the “Pacific Tuna and Ecosystem Research Cruise Project”, began in 2024 in collaboration with the FRA, the SPC and the IRD (Tawa et al., 2024). The main objectives of this research project are (1) to describe spatial and vertical distribution of larvae and juvenile skipjack, yellowfin and bigeye tuna, and its relationship with oceanographic features and the biological environment; and (2) to improve our understanding of the early survival and recruitment process in the Pacific Ocean. The detailed objectives and survey plan of this project were reported as an Information Paper to WCPFC-SC20 (Tawa et al., 2024), while the preliminary results of the KY2405 cruise were reported as an Information Paper to WCPFC-SC21(Tawa et al., 2025).

In the 2025 cruise, some observation stations in the equatorial region were relocated to 5°N based on the results of the 2024 cruise (Tawa et al., 2025); however, the overall research area remained largely unchanged. This document reports the preliminary results of the cruise conducted in 2025 as part of the research project. Although most of the results presented here are based on provisional information

obtained on board the vessel, some include analyses conducted on land as well as comparisons with results obtained during the KY2405 cruise.

Study Area and Sampling Design

The first leg (Leg 1) from Harumi in Tokyo to Honiara in Solomon Islands took place from 27 August to 28 September. It was set to survey an area spanning 170°E–170°W and 0°–5°N. The second leg (Leg 2) from Honiara to Saipan took place from 2 to 20 October. It surveyed a north-south line on the 150–160°E and 0–15°N (**Fig. 1**). A total of 16 monitoring stations were set up each leg. There are two types of station: "long" and "short", defined by the time spent on station. Intensive observations were conducted both at the long station (star in **Fig. 1**) for three days and at the short station for one day (solid circle in **Fig. 1**); long station differ from short station by including the use of the midwater trawl. The details of the monitoring stations and research contents are shown in **Table 1**.

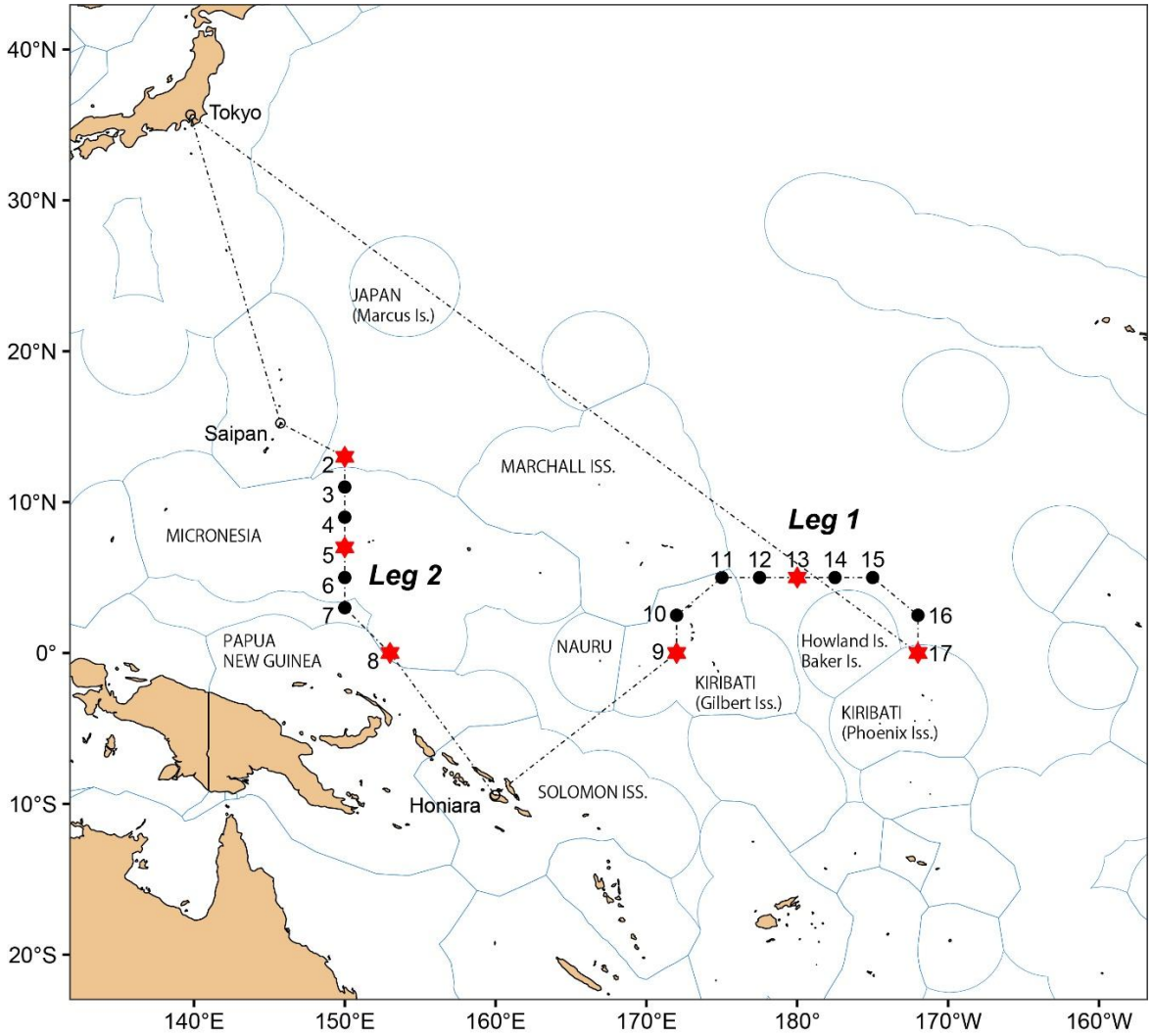

Fig. 1. All monitoring stations of KY2505 cruise, where midwater trawling, zooplankton sampling, acoustic survey and oceanographic monitoring were conducted, and actual cruise track. There are two types of station: "long" (red star) and "short" (circle). Long station (three days) differ from short station (one day) by including midwater trawl. The blue lines indicate the cruise tracks. Monitoring started at station 17 and ended at station 2.

Table 1 Summary of research information at each station. Abbreviation: ln long station _1 indication day 1, _2 indicate day 2, _3 indicate day 3; SST, Sea Surface Temperature; CTD, Conductivity Temperature and Depth probe; RN0.3, Ring net with 0.334 mm mesh; RN1.0, Ring net with 1.0 mm mesh; BG0.3, Bongo net with 0.3 mm mesh; BG0.1, Bongo net with 0.1 mm mesh; MOHT, Matsuda-Oozeki-Hu Midwater Trawl; Norpac, twin-type North Pacific standard net; VMPS, Vertical Multiple Plankton Sampler; WBAT, WideBand Autonomous Transceiver.

Leg	Station	Date	Lat	Lat_min	S/N	Lon	Lon_min	E/W	SST	CTD (m)	Sampling gear	Acoustic gear (m)
1	17_1	7-Sep	0	0.134	S	171	59.736	W	27.5	CTD (1500)	RN0.3, RN1.0, Norpac, Trawl	WBAT (800)
1	17_2	8-Sep	0	0.333	N	171	57.29	W	27.5	CTD (500)	MOHT, BG0.3, Trawl	WBAT (800)
1	17_3	9-Sep	0	0.317	S	171	59.069	W	27.6	CTD (500)	BG0.1, Trawl, VMPS	WBAT (250)
1	16	10-Sep	2	27.667	N	172	1.644	W	28.1	CTD (1500)	RN0.3, RN1.0, VMPS, Norpac, BG0.3, BG0.1, MOHT	WBAT (800)
1	15	12-Sep	4	59.861	N	174	59.244	W	28.9	CTD (1500)	RN0.3, RN1.0, VMPS, Norpac, BG0.3, BG0.1, MOHT	WBAT (800)
1	14	13-Sep	4	56.567	N	177	26.275	W	28.8	CTD (1500)	RN0.3, RN1.0, VMPS, Norpac, BG0.3, BG0.1, MOHT	WBAT (800)
1	13_1	14-Sep	4	59.915	N	179	59.906	E	29.0	CTD (1500)	RN0.3, RN1.0, Norpac, Trawl	WBAT (800)
1	13_2	15-Sep	4	56.744	N	179	57.27	W	28.9	CTD (500)	MOHT, BG0.3, Trawl	
1	13_3	16-Sep	5	0.535	N	179	59.669	E	29.0	CTD (500)	BG0.1, Trawl, VMPS	WBAT (250)
1	12	17-Sep	4	53.32	N	177	30.964	E	29.6	CTD (1500)	RN0.3, RN1.0, VMPS, Norpac, BG0.3, BG0.1, MOHT	WBAT (800)
1	11	18-Sep	5	0.98	N	175	0.08	E	28.8	CTD (1500)	RN0.3, RN1.0, VMPS, Norpac, BG0.3, BG0.1, MOHT	WBAT (800)
1	10	20-Sep	2	30.196	N	171	58.243	E	28.9	CTD (1500)	RN0.3, RN1.0, VMPS, Norpac, BG0.3, BG0.1, MOHT	WBAT (800)
1	09_1	21-Sep	0	0.557	S	171	59.741	E	28.7	CTD (1500)	RN0.3, RN1.0, Norpac, Trawl	WBAT (800)
1	09_2	22-Sep	0	0.161	S	172	1.657	E	28.8	CTD (500)	MOHT, BG0.3, Trawl	WBAT (800)
1	09_3	23-Sep	0	0.291	S	171	59.23	E	29.1	CTD (500)	BG0.1, Trawl, VMPS	WBAT (250)
2	08_1	4-Oct	0	0.687	S	153	0.342	E	30.0	CTD (1500)	RN0.3, RN1.0, Norpac, Trawl	WBAT (800)
2	08_2	5-Oct	0	1.231	N	153	4.833	E	30.1	CTD (500)	MOHT, BG0.3, Trawl	WBAT (800)
2	08_3	6-Oct	0	0.138	S	153	0.531	E	30.1	CTD (500)	BG0.1, Trawl, VMPS	WBAT (250)
2	07	9-Oct	2	59.089	N	150	8.883	E	30.3	CTD (1500)	RN0.3, RN1.0, VMPS, Norpac, BG0.3, BG0.1, MOHT	WBAT (800)
2	06	9-Oct	4	59.45	N	150	0.041	E	30.4	CTD (1500)	RN0.3, RN1.0, VMPS, Norpac, BG0.3, BG0.1, MOHT	WBAT (800)
2	05_1	10-Oct	7	0.399	N	150	0.219	E	30.2	CTD (1500)	RN0.3, RN1.0, Norpac, Trawl	WBAT (800)
2	05_2	11-Oct	7	4.718	N	149	59.309	E	29.9	CTD (500)	MOHT, BG0.3, Trawl	WBAT (800)
2	05_3	12-Oct	6	59.358	N	150	0.605	E	29.9	CTD (500)	BG0.1, Trawl, VMPS	WBAT (250)
2	04	14-Oct	8	55.583	N	149	48.123	E	30.0	CTD (1500)	RN0.3, RN1.0, VMPS, Norpac, BG0.3, BG0.1, MOHT	WBAT (800)
2	03	14-Oct	10	59.825	N	150	0.524	E	29.9	CTD (1500)	RN0.3, RN1.0, VMPS, Norpac, BG0.3, BG0.1, MOHT	WBAT (800)
2	02_1	15-Oct	13	0.239	N	149	58.941	E	29.9	CTD (1500)	RN0.3, RN1.0, Norpac, Trawl	WBAT (800)
2	02_2	16-Oct	12	57.036	N	149	59.347	E	29.7	CTD (500)	MOHT, BG0.3, Trawl	WBAT (800)
2	02_3	17-Oct	12	59.52	N	149	59.772	E	29.8	CTD (500)	BG0.1, Trawl, VMPS	WBAT (250)

Oceanographic observations

Vertical observations of water temperature, salinity, dissolved oxygen concentration and chlorophyll-a concentration were made using a CTD (SBE 911plus CTD, Sea-Bird) up to 1500 m depth. Nutrients and chlorophyll-a samples were collected from Niskin-X bottles and kept frozen until analyses on land. Nutrient concentrations were measured using a colorimetric method (QuAAtro39, BLTEC; Kodama et al. 2014), and chlorophyll-a concentrations were measured fluorometrically (Trilogy, Turner Designs; Welschmeyer 1994, Suzuki & Ishimaru 1990). Clustering was conducted using the Ward method for a Euclidean distance matrix calculated from standardized data comprising temperature, salinity, nitrate + nitrite and chlorophyll-a at 12 layers in 10–200 m depth.

Oceanographic condition

During the KY2505 cruise, there were three major surface currents in the study area (**Fig. 2a**): the westward-flowing North Equatorial Current (NEC) and South Equatorial Current (SEC) in the north and south parts of the transect, respectively, and the eastward-flowing North Equatorial Countercurrent (NECC) between NEC and SEC. Because of the Coriolis effect and these currents, divergence and convergence occurred in the study area (**Fig. 2b, c**). In addition, the eastward-flowing Equatorial Undercurrent (EUC) was observed below SEC. These features were generally similar to those observed in the KY2405 cruise. However, the eastward current was found above 100 m depth in 2–4 °N during this cruise, whereas the westward current was found in the same location during the KY2405 cruise.

The location of Leg1 stations was substantially modified from that of KY2405 cruise, and Stations 11–15 located at the convergence zone between SEC and NECC (**Fig. 2b**). Along the Leg1 transect, temperature increased northward and westward, and a warm pool-like conditions—where the surface temperature is higher than 29 °C—was observed at 3 northwestern stations (Stations 10–12; **Fig. 3a**). Salinity was generally higher than 35 in 0–150 m depth along the transect, except at stations where warm pool-like conditions were observed (**Fig. 3b**). Nitrate and nitrite concentrations above 100 m depth were relatively higher at stations on the equator (Stations 9, 17) than those at other stations, being especially depleted at Stations 11–12 (**Fig. 3c**). Chlorophyll-a concentrations were consistently higher than 0.2 µg L-1 within the upper 100 m layer along the transect, whereas obvious subsurface maxima were observed at warm pool-like stations around 50-100 m depths (Stations 11-12, **Fig. 3d**).

As for the Leg 2 south-north transect, hydrographic features were similar to those observed at the same location during the KY2405 cruise. Temperature was higher than 29 ℃ at the surface and generally decreased from south to north in 0−100 m depth (**Fig. 4a**). On the other hand, surface salinity was particularly lower than 34 in the central part of the transect (Stations 5-7) and high salinity water (>35) was observed at both edges of the transect. The thermocline became shallower at Station 4−6 below 100 m depth, corresponding to low-salinity water distribution. Nitrate and nitrite concentrations were depleted in the upper 100 m layer, but an elevation of nutricline was observed around Station 5, concurrent with the shallow thermocline (**Fig. 4c**). Although chlorophyll-a concentrations were consistently higher than 0.2 µg L-1 in 0–100m depth at Station 8, those decreased northward and obvious subsurface chlorophyll maxima were observed mostly below 100 m depth north of 3 °N (**Fig. 4d**).

Based on data about temperature, salinity, nitrate + nitrite and chlorophyll-a collected during the KY2405 and KY2505 cruise, cluster analysis was conducted and sampling stations were divided into 4 groups (**Fig. 5**). Stations 12–19 during KY2405 cruise and Stations 9–10, 16–17 during KY2505 cruise were classified into Equatorial upwelling region characterized by relative low temperature, high salinity and high nutrient and chlorophyll-a concentrations. Stations 4–7 during KY2405 cruise and Stations 4–6 during KY2505 cruise were classified into Subtropical region with high precipitation and divergence resulting in low salinity at the surface and elevation of both the thermocline and nutricline. Station 8 during KY2405 and Stations 7–8, 13–15 during KY2505 belonged to Subtropical region affected by equatorial upwelling, whereas the other stations were in Oligotrophic subtropical region. The results of KY2505 cruise were almost the same as those of KY2405 cruise, except for Station 7.

(a)

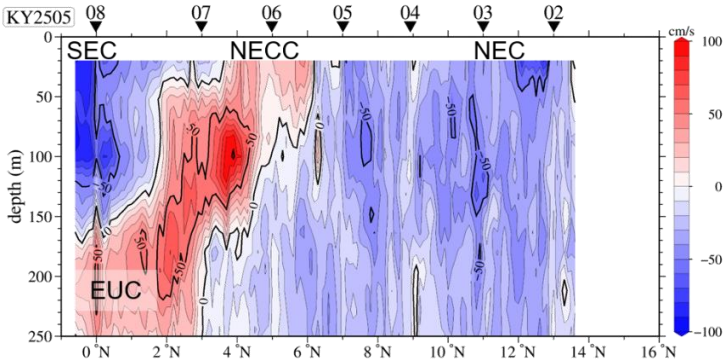

(b)

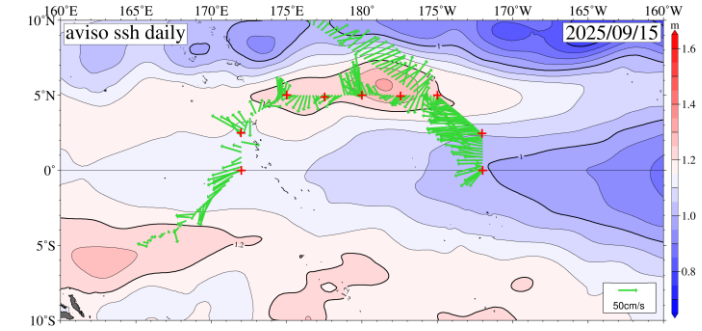

(c)

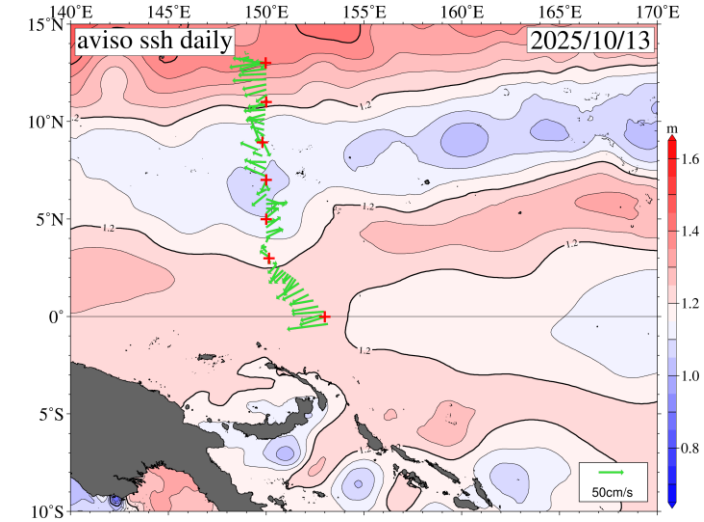

Fig. 2. (a) Current velocity (cm/s) along the Leg2 south-north transect measured by ADCP. Blue and red show westward and eastward flows, respectively. (b) Current velocity (green arrows) measured by ADCP and sea surface height (SEALEVEL_GLO_PHY_L4_MY_008_047. E.U. Copernicus Marine Service Information (CMEMS). Marine Data Store (MDS). https://doi.org/10.48670/moi-00148 (Accessed on 29 JUN 2026)) during Leg1 and (c) Leg2. Red plus symbols represent sampling stations during KY2505 cruise. Abbreviations represent major currents in the study area.
SEC: South Equatorial Current
NEC: North Equatorial Current
NECC: North Equatorial Countercurrent
EUC: Equatorial Undercurrent

(a) Temperature (°C)

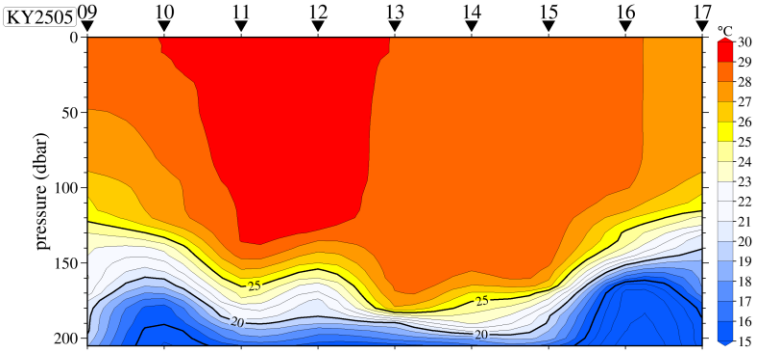

(b) Salinity

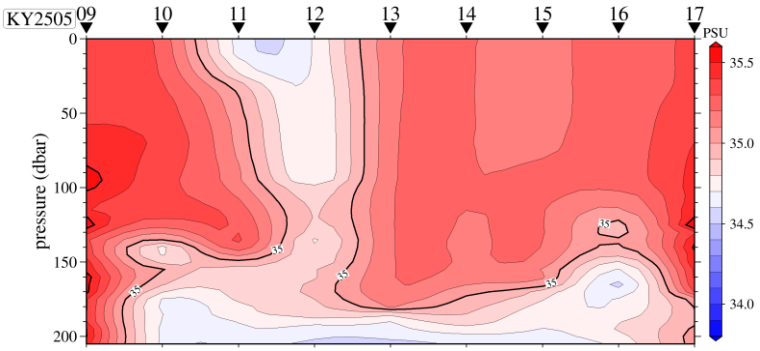

(c) Nitrate + nitrite (μM)

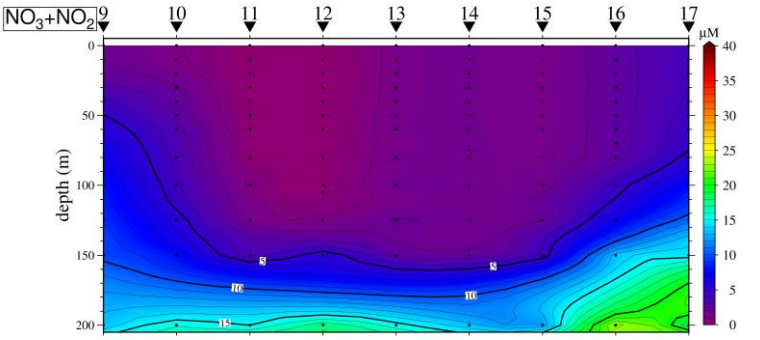

(d) Chlorophyll-a (μg / L)

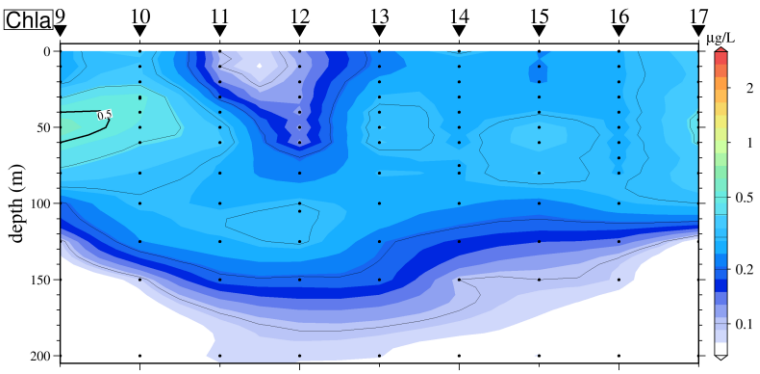

Fig. 3. (a) Temperature, (b) salinity, (c) nitrate + nitrite, and (d) chlorophyll-a concentration at 0–200 m depth along the Leg1 transect.

(a) Temperature (°C)

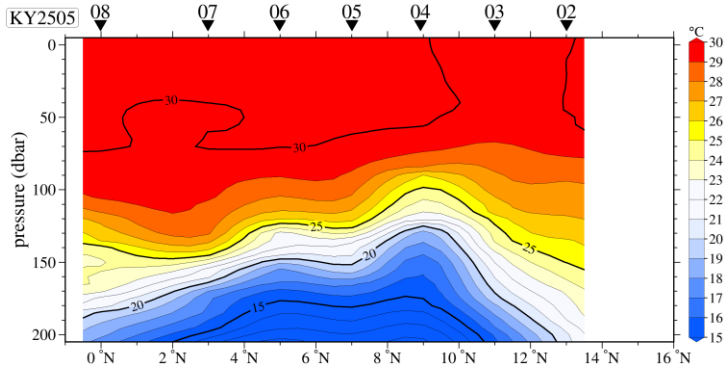

(b) Salinity

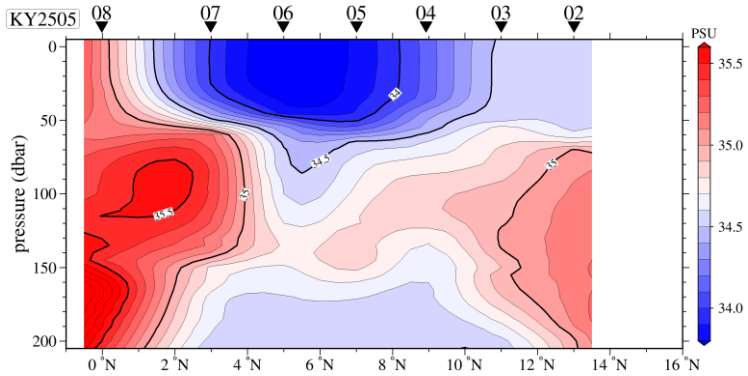

(c) Nitrate + nitrite (μM)

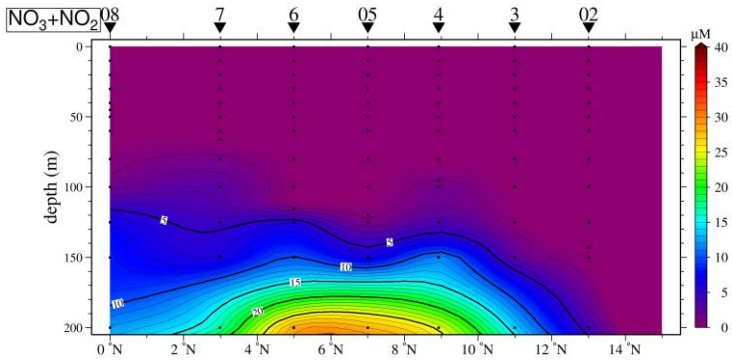

(d) Chlorophyll-a (μg / L)

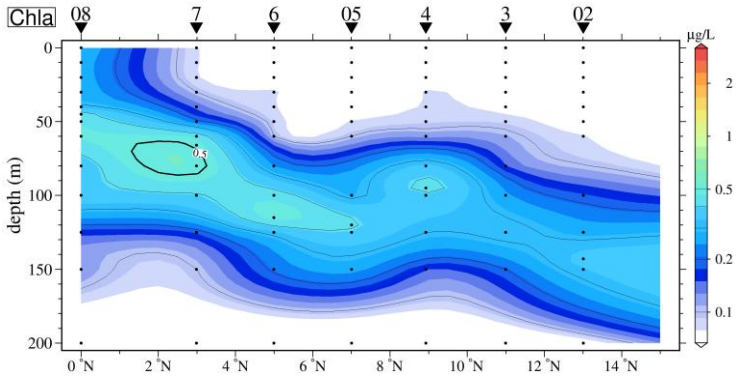

Fig. 4. (a) Temperature, (b) salinity, (c) nitrate+nitirite, and (d) chlorophyll-a concentration at 0–200 m depth along the Leg2 south-north transect.

(a)

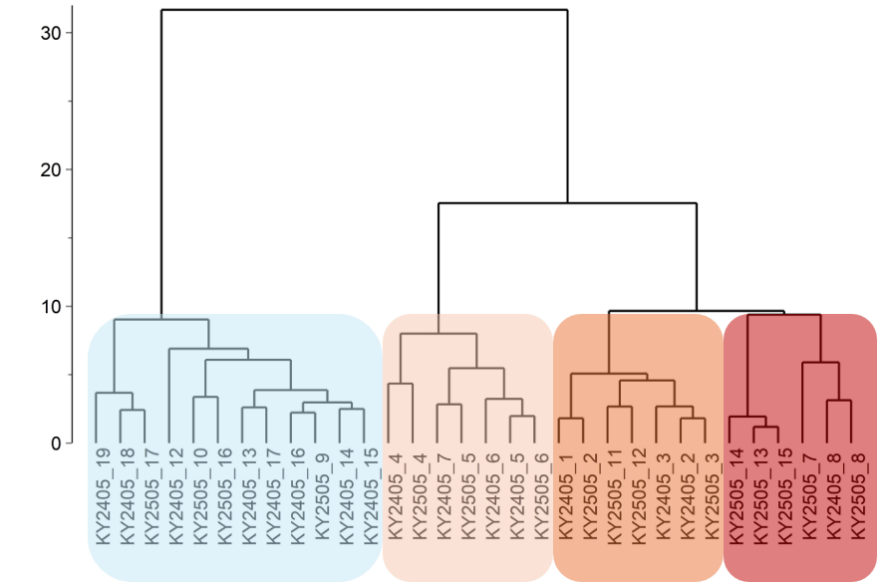

(b)

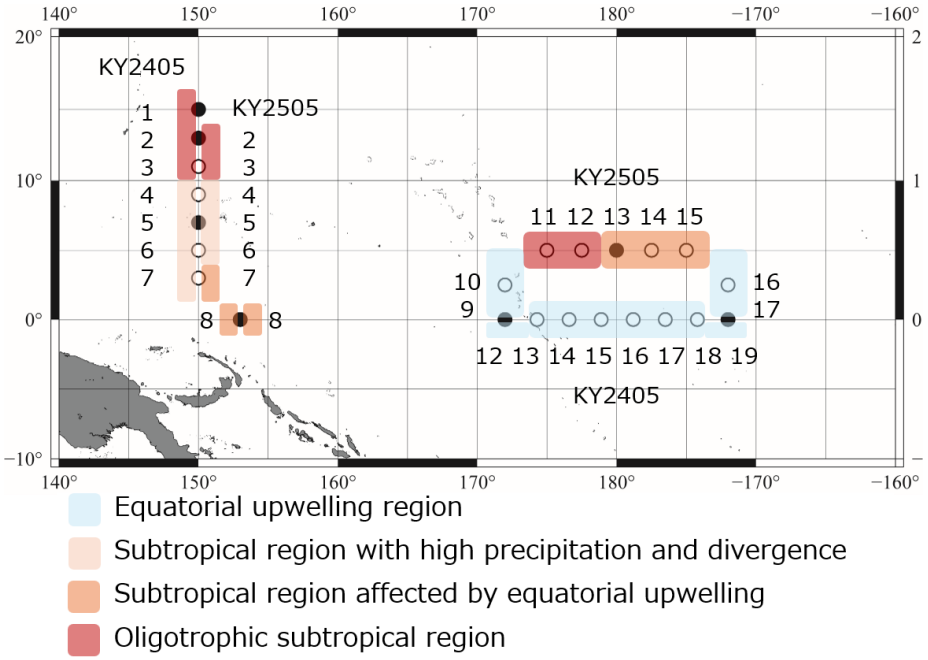

Fig. 5. (a) The result of cluster analysis of oceanographic conditions at each sampling station during KY2405 and KY2505 cruise. (b) Each group position distinguished by clusters in the study area.

Active acoustic echosounders

Assessment of the amount and size of biological organisms was completed by acquiring active acoustic data, both continuously and in station. Several instruments were deployed during the survey, including a Simrad EK80 hull-mounted split-beam echosounder, an Acoustic Doppler Current Profiler (ADCP), and a profiler WideBand Autonomous Transceiver (WBAT). All acoustic instruments emit echos at a given frequency and record the backscattered intensity, modulated by the obstacles encountered in the path of the acoustic wave (e.g. living organisms).

Hull-mounted echosounders, EK80 and ADCP, sample large volumes over various depth ranges (down to 1000 m, depending on the frequency) and help describe large scale water column patterns (e.g. vertical structuration, diel vertical migrations, differences across various ecosystems). ADCP specifically measures currents direction and velocity. Data with hull-mounted echosounders were collected continuously along the cruise. Conversely, the profiler WBAT was deployed only in stations (see **Fig. 6**). The profiler was sent into layers at depth, as close as possible to individual organisms to help counting and identifying them. The profiles reached 800 m to sample the mesopelagic layer. The sampling range of WBAT is small (40 m), ensuring that only a small number of distinct organisms are sampled. During the whole cruise (Leg 1 & 2 together), a total of 28 vertical profiles were acquired with the WBAT.

According to the frequency they operate, echosounders observe different kinds of organisms. In general, the higher the frequency used, the smaller the detected targets. Thus, low frequencies (≤ 120 kHz) are adapted to micronekton (2-20 cm organisms) while high frequencies (> 120 kHz) are more suited for the study of zooplankton. The WBAT operated at 38 and 120 kHz, targeting micronektonic organisms, while the EK80 operated at 38, 70, 120, and 200 kHz, enabling the observation of wider range of organisms.

Because of their different characteristics (acquisition range, continuous vs punctual sampling, frequency), EK80 and WBAT provide complementary images of the ecosystem. Together, they show both fine-scale details at stations (local assemblages and density) and large-scale patterns in the ocean (biologic layers, consistent ecoregions).

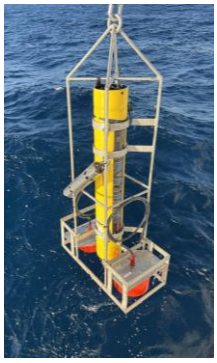

Fig. 6. The profiler WBAT in its frame, equipped with 2 transducers (38 and 120 kHz) and a depth sensor (TDR).

Hull-mounted echosounders (EK80)

The EK80 data were acquired at 4 frequencies 38, 70, 120 and 200 kHz, at ranges down to 1000, 700, 300 and 200 m, respectively. Acoustic data was emitted every 4 seconds, alternately with ADCP data. The Mean Volume Backscattering Strength (MVBS or Sv in dB re 1 m^{-1}) integrated over the water column is plotted in **Fig. 7** for the four frequencies. This representation highlights the spatial variability of acoustic density across the entire survey area. At the lower frequencies (38 and 70 kHz), the eastern areas (longitude > 170°E) around the equator (latitude < ±5°) presented high acoustic densities (MVBS > −75 dB re 1 m^{-1}), suggesting a productive area in the equatorial upwelling region. In contrast, the

northwestern transect (Leg2: ~150°E / 5°-15°N) displayed lower acoustic densities decreasing when moving away from the equator, across all four frequencies (MVBS < −80 dB re 1 m^{-1}), indicative of relatively weak scattering layers in this area. At higher frequencies (120 and 200 kHz), the spatial patterns were broadly consistent with those observed at lower frequencies, with high densities concentrated in the eastern equatorial region. However, their reduced integration depth, limited to the epipelagic layer (< 250 m), only captured a fraction of the water column, partly explaining the greater spatial heterogeneity observed compared to 38 and 70 kHz. The higher frequencies also revealed a distinct area of high MVBS around 172–175°E- 4°N, which was not as clearly defined at 38 and 70 kHz.

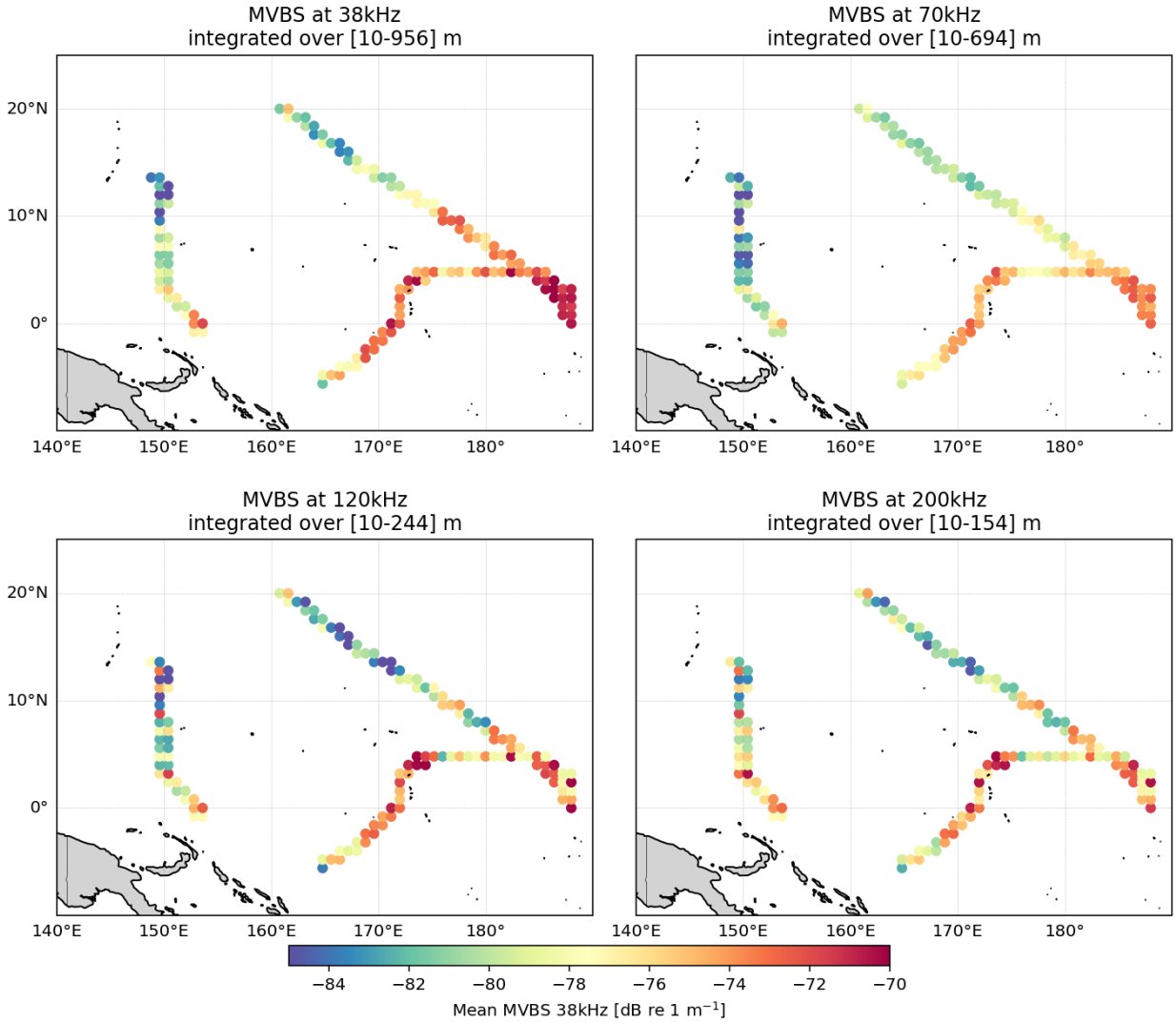

Fig. 7. Depth-integrated mean volume backscattering strength (MVBS, dB re 1 m^{-1}) at 38 kHz (10–956 m), 70 kHz (10–694 m), 120 kHz (10–244 m) and 200 kHz (10–154 m) averaged over 0.8°×0.8° grid cells across the survey area. The colorbar is shared across all four frequencies.

Overall, the spatial distribution of integrated acoustic density suggested a clear contrast between the oligotrophic northwestern waters and the more productive equatorial region, consistent with known oceanographic gradients in the western and central Pacific. Two 24-hours examples of vertical echograms between the surface and maximum depth range of the four frequencies are presented in **Fig. 8: A)** in the higher MVBS density from Leg1 and **B)** the lowest values of Leg2. The diel vertical migration (DVM) is visible with organisms ascending to the surface layer at night and descending to 300-600 m during the day. These strongly contrasted areas confirmed that acoustics is a useful tool for

ecosystem classification at large scale.

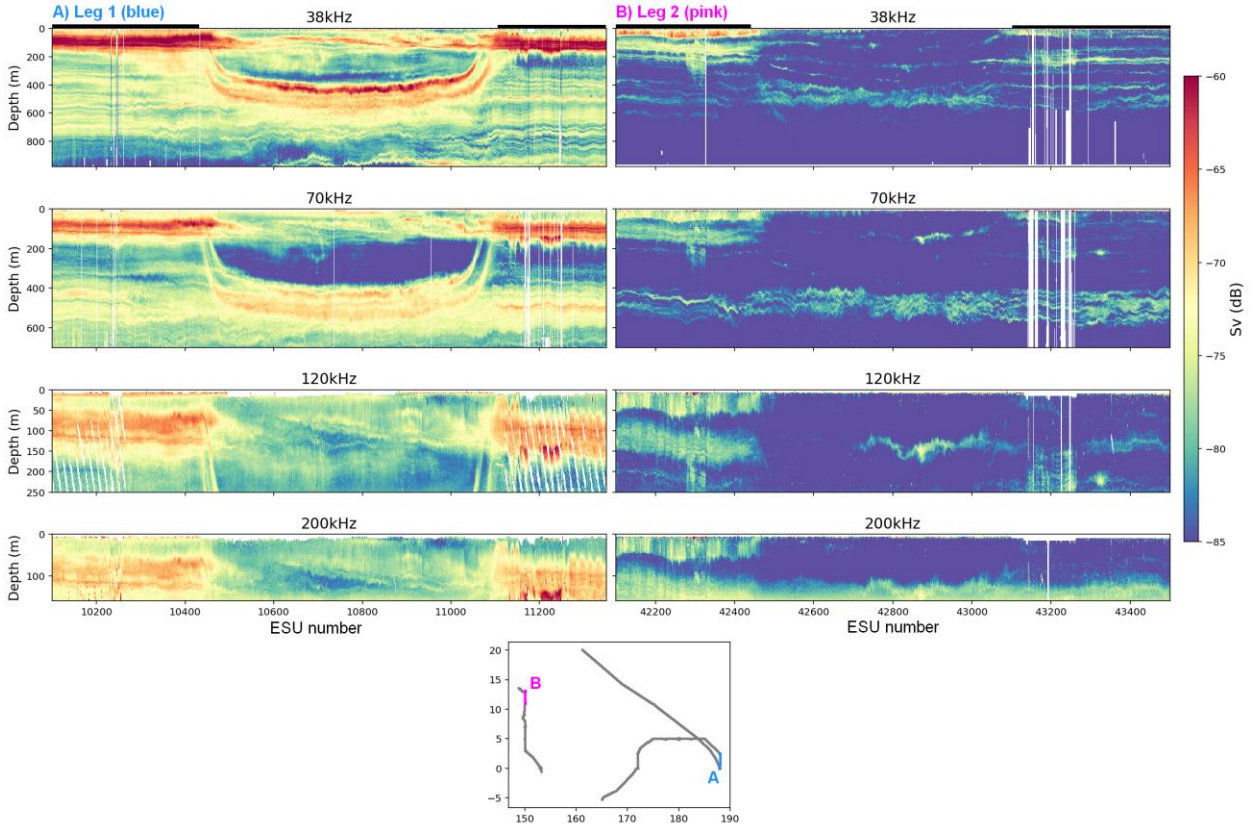

Fig. 8. Volume backscattering strength (Sv, dB re 1 m^{-1}) echograms at 38, 70, 120 and 200 kHz for two contrasted areas sampled during KY2505: **A)** Leg 1 (blue, equatorial region) and **B)** Leg 2 (pink, northwestern transect), as indicated on the inset map. For each area, echograms are displayed as a function of depth and Elementary Sampling Unit (ESU) number over a 24-hour period, with nighttime indicated by the black horizontal bar at the top of each panel. Note that depth ranges differ between frequencies. All the graphics share a common colorbar.

Ecosystems classification with acoustic profiles

To characterize the pelagic ecosystems sampled during KY2505, we applied a hierarchical Ward classification to the concatenated day and night MVBS profiles at 38 and 70 kHz, averaged over 2°×2° grid cells. Day and night profiles were averaged separately and concatenated vertically in each cell. This approach yielded four distinct acoustic clusters (**Fig. 9a, b, c**). The dendrogram (**Fig. 9b**) revealed a classification with two main branches: a group with low MVBS values comprising Cluster 0 (blue) and Cluster 2 (red), and an eastern equatorial group comprising Cluster 1 (green) and Cluster 3 (orange). The spatial distribution of clusters (**Fig. 9a**) showed a coherent geographic pattern: Cluster 0 was confined to the northwestern transect of Leg2 (~150°E, 5–15°N), while Clusters 1 and 3 dominated the subequatorial region (latitude $<$ 6°N). Cluster 2 occupied the northeastern area, corresponding to the North Pacific Gyre. The mean vertical profiles at 38 kHz (**Fig. 9c**) showed that Cluster 0 was characterized by low backscatter throughout the water column, with little difference between day and night profiles, suggesting weak or absent diel vertical migration (DVM). Cluster 3 located in the equatorial upwelling zone, displayed the highest acoustic densities and a pronounced DVM signal. Cluster 1 exhibited a similar pattern to Cluster 3 but with overall lower MVBS values, suggesting a less productive but dynamically similar ecosystem. Finally, Cluster 2 was distinguished by low daytime backscatter throughout the water column, including in the mesopelagic layer (> 400 m), and a strong nocturnal scattering layer in the epipelagic zone (0-200 m), with little change in the mesopelagic at night.

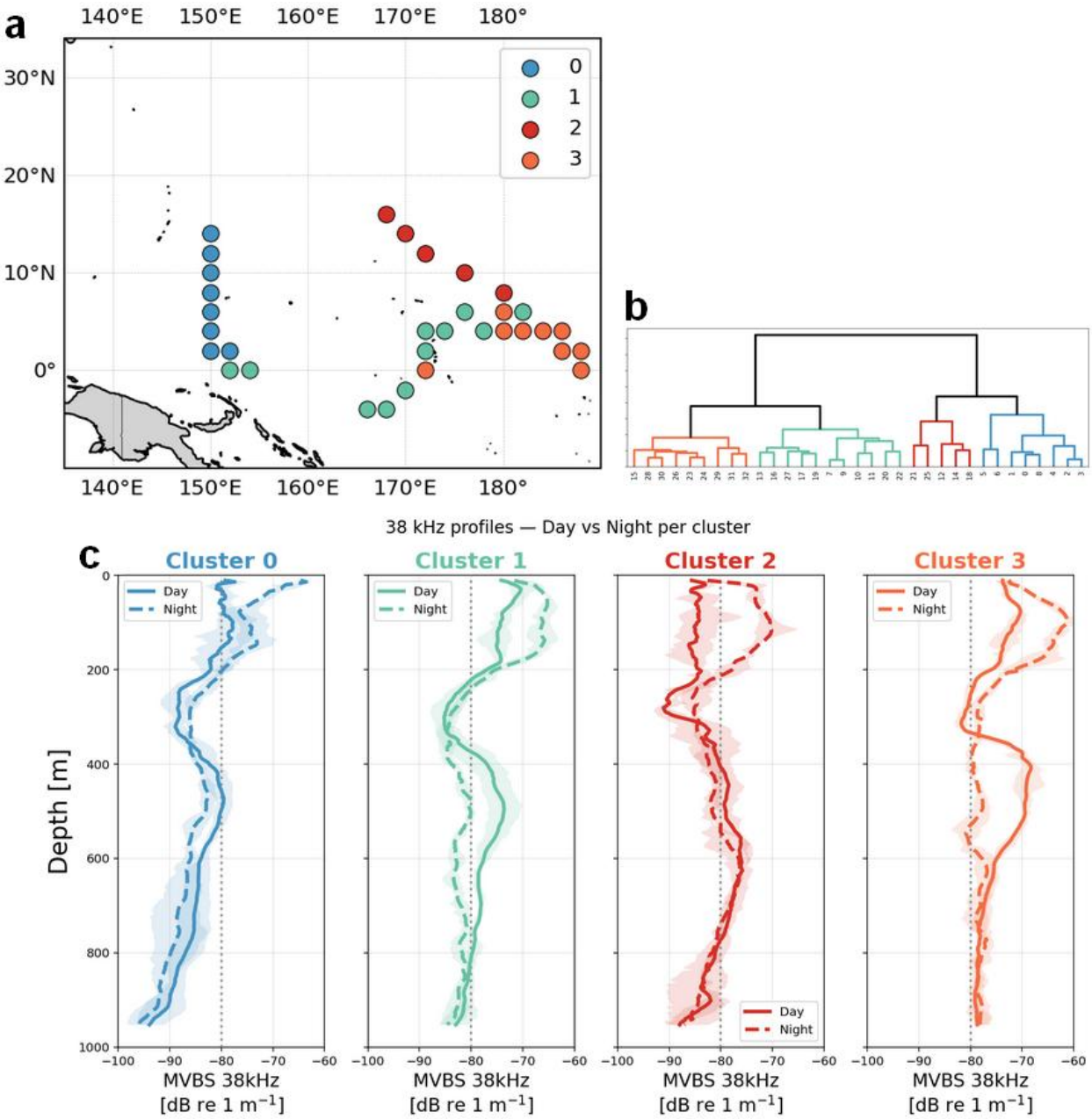

Fig. 9. Hierarchical classification of acoustic profiles from the KY2505 survey into four clusters. **a)** Spatial distribution of the four clusters across the survey area. Each dot represents a 2°×2° grid cell colored according to its cluster assignment. **b)** Dendrogram resulting from the Ward linkage hierarchical classification applied to the concatenated day and night MVBS profiles from 38 and 70 kHz. Branch colors correspond to the four clusters identified at the selected cut level. **c)** Mean (solid line: day; dashed line: night) and interquartile range (shaded area) of 38 kHz MVBS profiles for each cluster, displayed as a function of depth (0-1000 m). The vertical dotted line at -80 dB is shown as a reference for inter-cluster comparison.

Interannual classification (KY2405 vs. KY2505)

To assess the interannual consistency of the identified acoustic ecosystems, the classification was applied to the concatenated dataset from both KY2405 and KY2505 surveys (**Fig. 10**). The spatial distribution of the four clusters (**Fig. 10a**) was broadly consistent between years, with a similar geographic structure found across both surveys. The equatorial and subequatorial regions were occupied

by Clusters 0 and 2 (blue and red). Cluster 1 (green) dominated the classification of KY2405 between 3° and 25°N. Cluster 3 (orange) was found in KY2505 during Leg2 (transect ~150°E), separating this region from the rest of the oligotrophic areas of Cluster 1 (green). The dendrogram (**Fig. 10b**) reproduced the same two-branch structure as the single-survey classification, with the deepest split separating a western/northern group from an eastern/equatorial group. The equatorial cells were separated from the rest within the left branch, confirming the persistent and distinctive acoustic signature of this zone across both years.

However, some interannual differences were apparent. In KY2405, Cluster 1 (green) dominated a large portion of the survey area, from the northwestern transect down to the equatorial region, whereas in KY2505 this cluster was more restricted spatially. Cluster 3 (orange) covered all of Leg2 transect in KY2505, suggesting a shift in acoustic conditions in this area between the two surveys. These differences may reflect interannual variability in oceanographic conditions in the tropical regions, like ENSO phase.

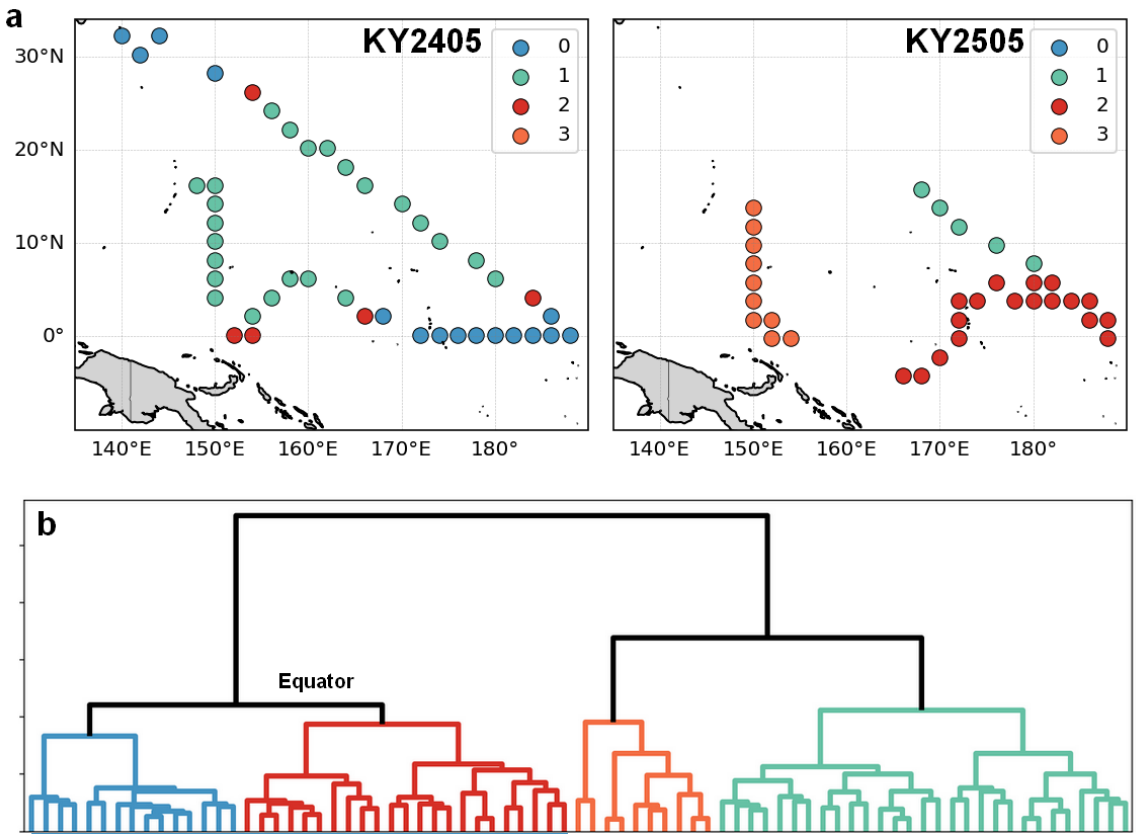

Fig. 10. Hierarchical classification of acoustic profiles from the combined KY2405 and KY2505 surveys into four clusters. **a)** Spatial distribution of the four clusters in each survey (KY2405, left; KY2505, right). Each dot represents a 2°×2° grid cell colored according to its cluster assignment. **b)** Dendrogram resulting from the Ward linkage hierarchical classification applied to the concatenated day and night MVBS profiles from 38 and 70 kHz. Branch colors correspond to the four clusters identified at the selected cut level. The "Equator" label indicates the node at which the equatorial grid cells are separated from the rest within the left branch of the dendrogram, highlighting the distinctive acoustic signature of the equatorial zone.

Acoustic profilers

WBAT profiles were conducted during daytime, nighttime, and sunset periods to characterize temporal changes in organism vertical distribution and investigate diel vertical migration. The mean volume backscattering strength (MVBS), which is the average acoustic intensity recorded by the WBAT,

was used as a proxy of organism density. At Station 17 (0°N, 172°W), distinct scattering layers were observed during both day and night (**Fig. 11**). A deep scattering layer (DSL) was present between 300 and 500 m during daytime, while a surface scattering layer (SSL) dominated the upper 200 m at night, consistent with the expected diel migration pattern. Similar distributions were observed at both 38 and 120 kHz. Despite the pronounced DSL during daytime, the SSL remained clearly detectable, with MVBS values comparable to those of the DSL (approximately −60 dB), suggesting the presence of resident epipelagic organisms that do not participate in the migration.

Sunset profiles were specifically designed to monitor the upward migration of organisms. To maximize the probability of intercepting migrant layers, the profiler stopped at 250 m depth. This depth, corresponding to the typical position of the migrant layer, was fixed empirically during the cruise. Acoustic observations revealed several successive increases in backscatter intensity (three migration waves in **Fig. 11**), interpreted as distinct cohorts of migrating organisms crossing the acoustic beam. The predominantly upward trajectories of organisms observed within these waves support the interpretation that they are migrating.

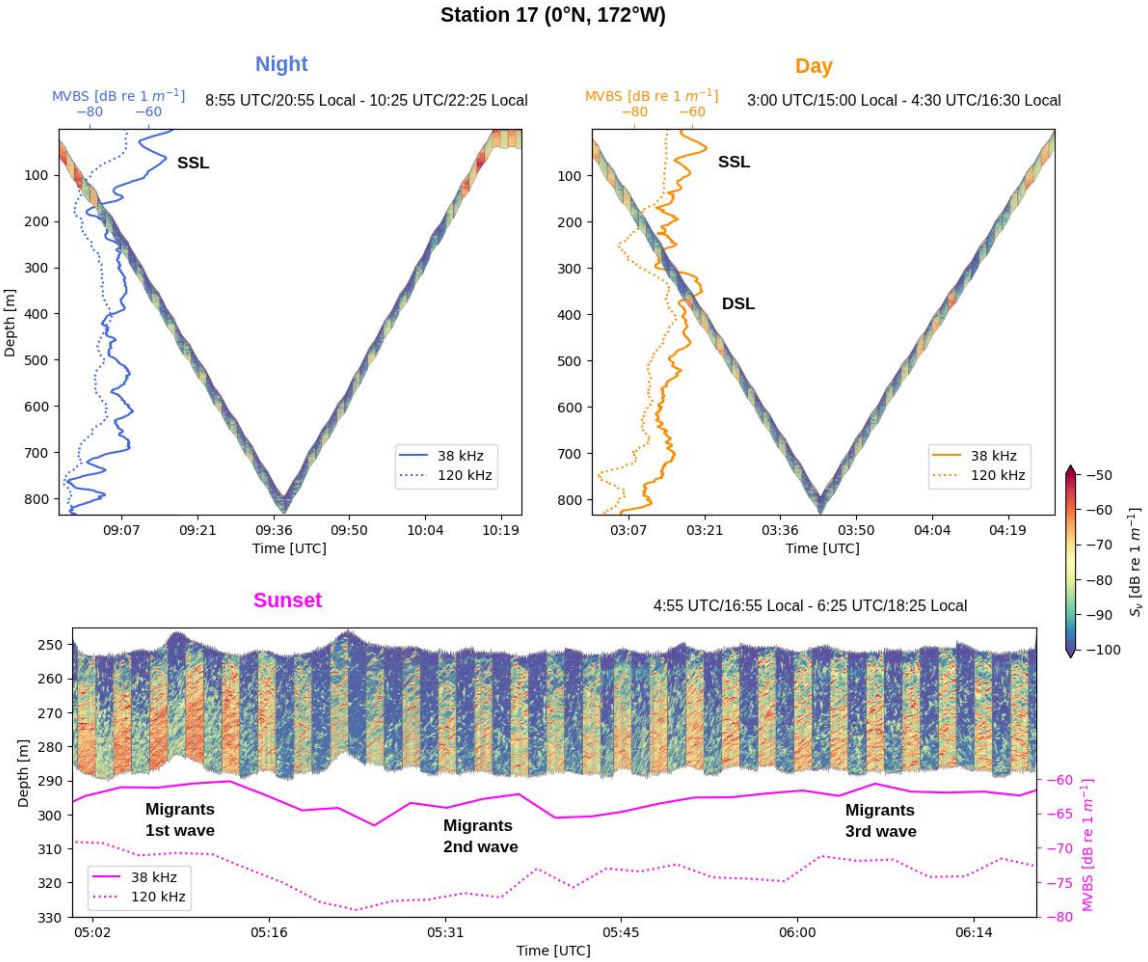

Fig. 11. WBAT profiles at station 17 (0°N, 172°W). Echograms give the acoustic intensity (Sv) as a function of depth and time at night (left), day (right) and sunset (bottom). The acoustic intensity was averaged (MVBS) on 1m depth bins (top) and 1 minute time bins (bottom) and detailed for 38 and 120 kHz.

Acoustic intensity as a proxy for zooplankton biomass

Zooplankton was sampled at nighttime using a Vertical Multiple Plankton Sampler (VMPS), a net equipped with an opening-closing system allowing the sampling of several depth layers. Four depth

layers were chosen to anticipate a higher concentration of plankton close to the surface at night: 0–100, 100–200, 200–400, and 400–600 m. The mesh size, 100 µm, permitted the sampling of micro and meso-zooplankton. The volume of water filtered by each net was measured using an embedded flowmeter. Collected samples were preserved in 5% formalin. The wet weight was determined using a 80 µm filter and a scale at 0.001g.

Wet weight, relative to the filtered seawater volume, was globally higher in the western transect (LEG 2, 150°E). Highest wet weights were found in stations 9 and 11, with 57.8 mg/m^3 and 67.9 mg/m^3, respectively (see **Fig. 12** left). The zooplankton biomass was essentially concentrated in the first 200 m, with an average of 107.3, 29.7, 9.1 and 8.3 mg/m^3 for layers 0-100, 100-200, 200-400 and 400-600 m, respectively (see **Fig. 12** right). This distribution can be explained by the euphotic zone and diel vertical migrations.

Acoustic backscattering intensity is widely used as a proxy for biomass. Since VMPS and EK80 were sampling at the same time, the relationship between wet weight and backscattered intensity (Sv) was investigated. The median Sv at 200 kHz, a frequency sensitive to zooplankton-sized targets, was computed on the same depth layers than VMPS samplings. Wet weight (relative to filtered volume), was put into a logarithmic scale, to match the logarithmic scale of acoustic intensity in decibels. A moderate but significant correlation between median Sv and wet weight was observed ($r^2 = 0.48$, $p < 0.01$), see **Fig. 13**. The Sv remains a first approximation of the biomass, as acoustic backscattering depends not only on organism abundance, but also on morphology, orientation and composition of individuals.

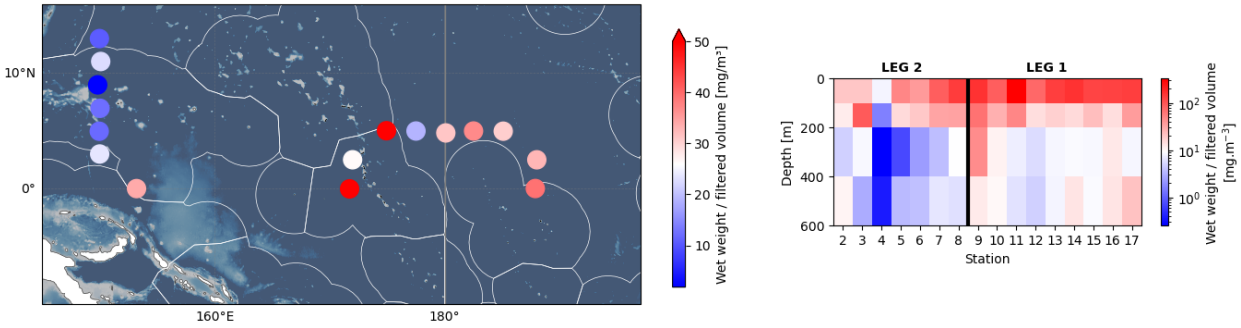

Fig. 12. Geographical and vertical variation of wet weight. Left: Wet weight (relative to filtered volume) integrated between the surface and 600m. The color scale was limited to 50 mg/m^3 because the station 11 (5°N, 175°E) showed a wet weight of 67.9 mg/m^3, erasing the variability among other stations (average wet weight = 28,6 mg/m^3). Right: the wet weight was detailed for each depth layers sampled by the VMPS. The values range between panels is very different because of integration ΣWW_i / ΣV_i at left.

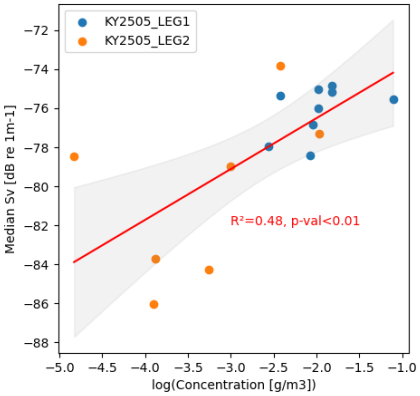

Fig. 13. Linear regression between median Sv at 200 kHz and wet weight (relative to filtered volume) in logarithmic scale.

Collection of Biological samples

A stratified collection was conducted using a twin-type North Pacific standard (NORPAC) net and a Vertical Multiple Plankton Sampler (VMPS) to sample the zooplankton that could be the food of tuna larvae. The zooplankton sampling by NORPAC net (mouth diameter, 0.45 m and mesh size, 0.1 mm) was conducted by vertical tow from 200 m depth to the surface. One of the samples collected was fixed in 5% formalin, the other was frozen. Sampling by the VMPS (mouth size, 0.5×0.5 m and mesh size, 0.1 mm) was conducted by a vertical tow at four layers: 600–400, 400–200, 200–100 and 100–0 m. VMPS samples were frozen to conduct isotope analysis. The volume of water filtered by the NORPAC net and VMPS was estimated with a mechanical flowmeter installed at the mouth of the net respectively.

Two types of ring net (mouth diameter; 2.0 m, mesh size; 0.334 and 1.0 mm) were towed horizontally in the surface layer to investigate the distributions of tuna larvae. Two types of bongo nets (mouth diameter; 0.70 m, mesh size; 0.334 mm and 0.1 mm) was also towed obliquely at the different layers, 60–40, 40–20 and 20–0m by 0.334 mm mesh and 200–0 m by 0.1 mm mesh.

Additionally, to investigate the vertical distribution of tuna larvae and early juvenile, Multiple layer Opening/Closing Matsuda-Oozeki-Hu Midwater Trawl (MOC-MOHT, Oozeki et al., 2012) with five net of a mouth area of 4 m^2 and a square mesh of 1.95 mm bar length (1.59 mm square pores) were conducted by oblique tow at four different depth layers, 120–90, 90–60, 60–30, 30–0 m. The towing time for each layer is 10 minutes, and the ship speed is 3.0 knots. A scanmar is attached to the net mouth to monitor the depth in real time. SBT500 was attached to obtain depth and water temperature on the tow net layers. The volume of water filtered by the MOC-MOHT was estimated with a mechanical flowmeter installed at the mouth of the net.

Midwater trawl operations using a NET-240 with a net mouth height of ca. 30 m and a cod end mesh size of <10 mm were conducted at six predetermined depth layers, 180, 150, 120, 90, 60 and 30 m to collect juvenile tropical tuna (skipjack, yellowfin and bigeye). In addition, an oblique tow between 200 m depth to surface was conducted (200–0 m). The survey was carried out over three days at each of the long stations (St. 02, 05, 08, 09, 13, 17). On Day 1, trawling was conducted twice in the deep depth zone (180 and 150 m); on Day 2, in the intermediate depth zone (120 and 90 m); and on Day 3, in the shallow depth zone (60 and 30 m) and oblique tow (200-0 m). The trawl duration was 30 minutes for each of the predetermined six depth layers, with no specific time limit for the oblique tow. To monitor the net depth and water temperature, a net monitoring device (Scanmar) and SBT500 loggers were attached to the trawl net and otter boards. The collected samples were sorted on board, as far as practicable, by species or major taxonomic group.

Scombrid larvae collected by three type plankton nets

A total of 96 larval net surveys were conducted during research period using ring nets (16 tows each mesh size, 0.334 and 1.0 mm), bongo net (48 tows at 0.334 mm mesh) and MOC-MOHT (16 tows). As a preliminary result of sorting, the numbers of tuna larvae and juveniles collected with these gears were 595 *Thunnus* spp., 552 *Katsuwonus pelamis*, 1 *Auxis thazard* and 13 unidentified scombrid larvae. Based on morphological observations and DNA analyses of a subset of the specimens, *Thunnus* spp. was found to comprise *Thunnus albacares*, *Thunnus obesus*, and *Thunnus alalunga*. Analyses of the remaining specimens are currently underway.

Figure 14 shows the horizontal distributions of *Thunnus* spp. and *K. pelamis* larvae collected during two types of ring net surveys. The larvae of both *Thunnus* spp. and *K. pelamis* were widely distributed in research areas on KY2505 cruise (**Figs. 14, 15**). During the KY2505 cruise, the highest density of *Thunnus* spp. larvae was observed at the southernmost station of Leg 2, located on the equator. In addition, *Thunnus* spp. larvae occurred at relatively high densities along the east–west transect at 5°N during Leg 1. In contrast to the KY2405 cruise, when *Thunnus* spp. larvae were rarely observed along the equatorial east–west transect in Leg 1, the KY2505 cruise showed generally higher larval densities throughout the study area. During the KY2505 cruise, *K. pelamis* larvae occurred at relatively high

densities at the station on 180°E during Leg 1 and at the equatorial station during Leg 2. In contrast to the KY2405 cruise, no exceptionally high densities (>100 individuals per 1,000 m³) were observed during the KY2505 cruise.

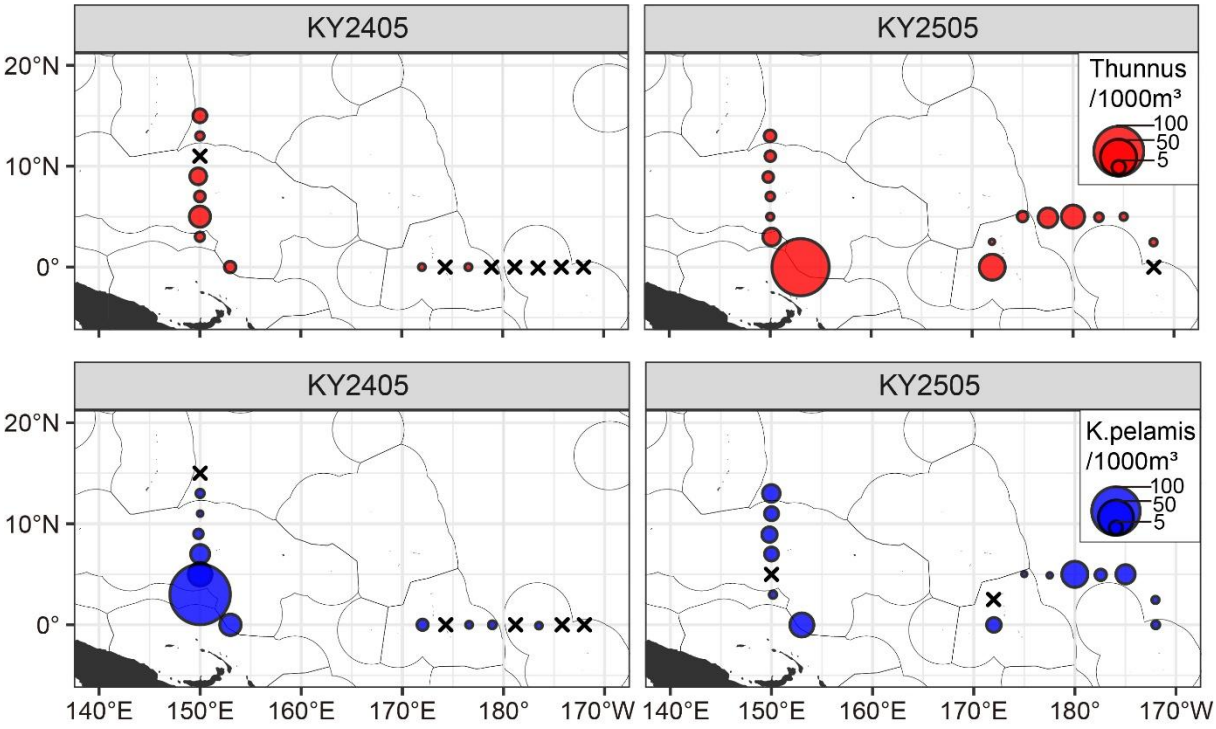

Fig. 14. Horizontal distribution of larvae of *Thunnus* spp. and *Katsuwonus pelamis* collected by two types ring nets. Larval density was estimated as the number of individuals per 1,000 m³ of filtered seawater using flowmeter measurements.

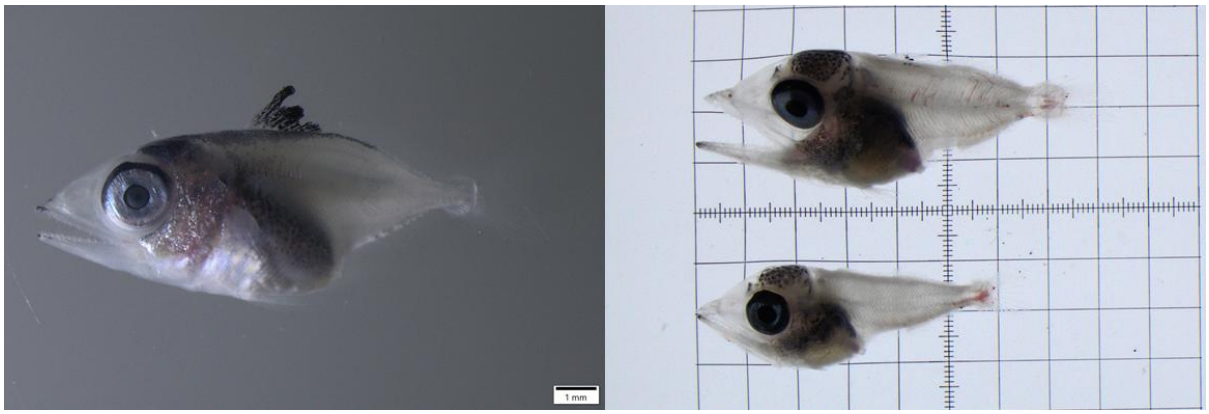

Fig. 15. Larvae of *Thunnus* sp. collected by ring net（Left: 10.7mmSL, RN0.3, St.12）and *Katsuwonus pelamis* (right upper; 7.1mmSL, right down; 5.8mmSL, RN1.0, St.14)

Figure 16 shows the size distributions of *Thunnus* spp. and *K. pelamis* larvae collected during two types of ring net surveys. The body lengths of *Thunnus* spp. and *K. pelamis* larvae collected by ring net surveys during the KY2505 cruise averaged 5.4 ± 1.2 mm (range: 3.2–8.6 mm) and 4.9 ± 1.1 mm (range: 2.7–8.7 mm), respectively. *Thunnus* spp. larvae exhibited a unimodal size distribution with a mode at approximately 5 mm, whereas *K. pelamis* larvae showed a bimodal distribution with modes at approximately 3 mm and 5 mm. Compared with the larval size compositions collected by ring net surveys during the KY2405 cruise, fewer small *Thunnus* spp. larvae (<4 mm) were collected during the

KY2505 cruise, while larvae around 5 mm in length and those larger than 9 mm were more abundant. In contrast, no marked differences in the size composition of *K. pelamis* larvae were observed between the two cruises.

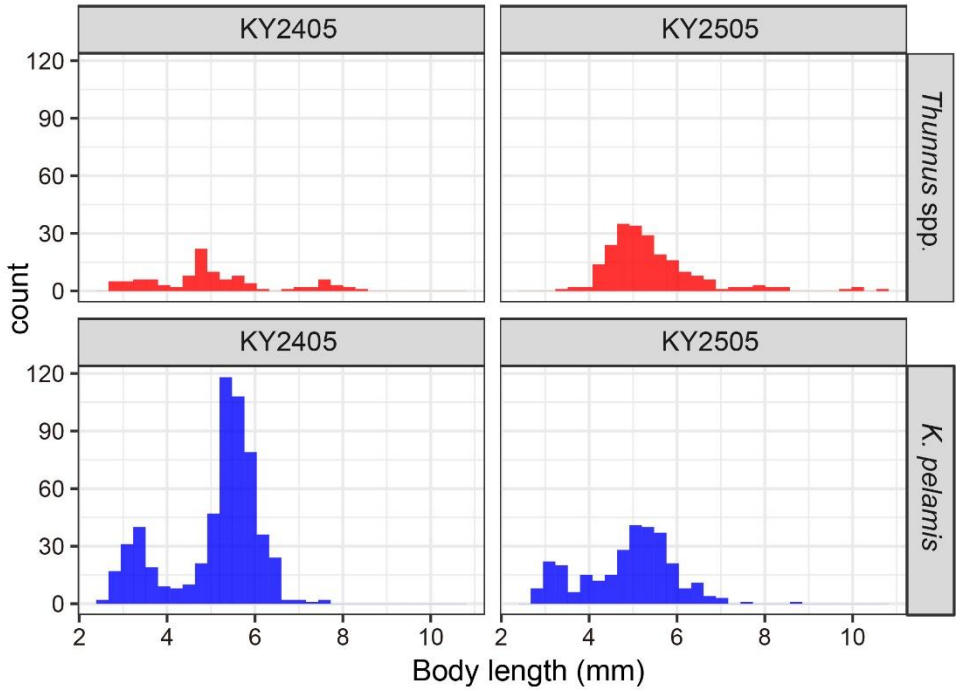

Fig. 16. Body length (notochord or standard length) of the larvae of *Thunnus* spp. and *Katsuwonus pelamis* collected by two types ring nets

Juvenile distribution by stratified midwater trawls surveys

A further 87 juvenile tuna was collected using a midwater trawl at different depths (**Table 2**). During each of Legs 1 and 2, 21 midwater trawl tows were conducted at three stations. Species identification based on morphological observations and DNA analyses showed that the collected scombrid juveniles comprised 25 *K. pelamis*, 2 *T. albacares* and 4 *T. obesus* in Leg 1 and 53 *K. pelamis* and 1 *T. albacares* and 1 *T. alalunga* in Leg 2 (**Table 2, Fig. 17a**). During the KY2505 cruise, relatively few *Thunnus* juveniles were collected, and no distinct distribution pattern was evident. In contrast, *K. pelamis* juveniles showed a tendency to occur in higher abundance at the equatorial stations (Stns. 08, 09, and 17) throughout the survey period.

Table 2 Total number of scombrid juveniles collected by midwater trawl at each station

Leg	Stn	*Katsuwonus pelamis*	*Thunnus albacares*	*Thunnus alalunga*	*Thunnus obesus*
1	17	10	2	0	0
1	13	0	1	0	0
1	09	15	0	0	4
2	08	46	0	0	0
2	05	2	1	0	0
2	02	5	0	1	0
	Total	78	4	1	4

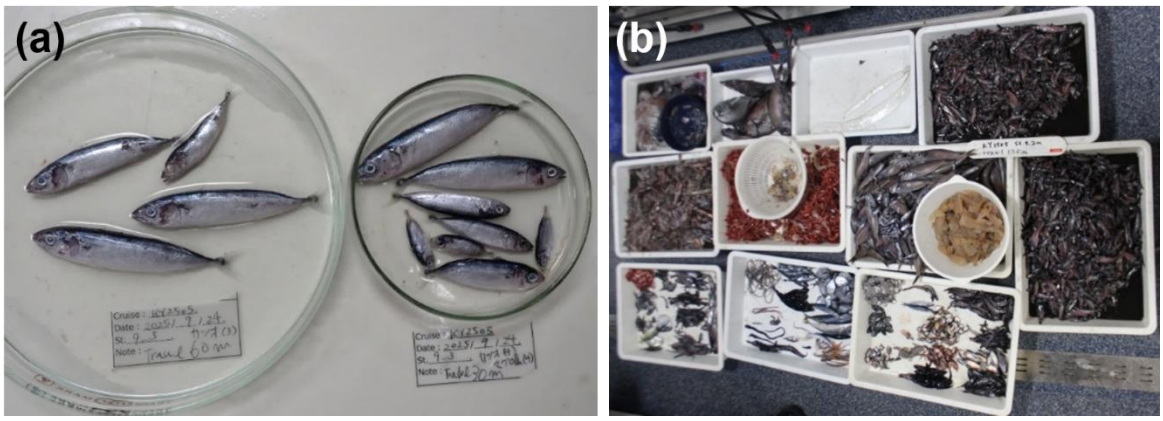

Fig. 17. Photographs of specimens collected by midwater trawl. (a) Juvenile *Katsuwonus pelamis* and *Thunnus obesus* collected at 30 and 60 m depth at Stn. 9. The four individuals on the left and the upper four on the right are *K. pelamis*, while the lower four on the right are *T. obesus*. (b) All specimens collected at 120 m depth at Stn. 9.

The average and range standard length of *K. pelamis* was 55.1 ± 18.9 (15.0–124.2) mm, that of *T. albacares* was 59.0 ± 30.7 (28.3–106.3) mm, that of *T. obesus* was 33.2 ± 9.3 (27.7–49.4) mm and that of *T. alalunga* was 46.0 mm. **Figure 18** shows the abundance and size composition of *K. pelamis* collected by depth-stratified midwater trawl tows. During the KY2505 cruise, the highest abundance of *K. pelamis* juveniles was recorded in tows centered at a depth of 120 m, whereas abundances at other depth strata were relatively similar. In contrast, during the KY2405 cruise, the greatest number of *K. pelamis* juveniles was collected at the shallowest depth (30 m), and relatively high abundances were also observed at depths of 70 m and 130 m. The mean body length of *K. pelamis* juveniles did not vary substantially among depth strata.

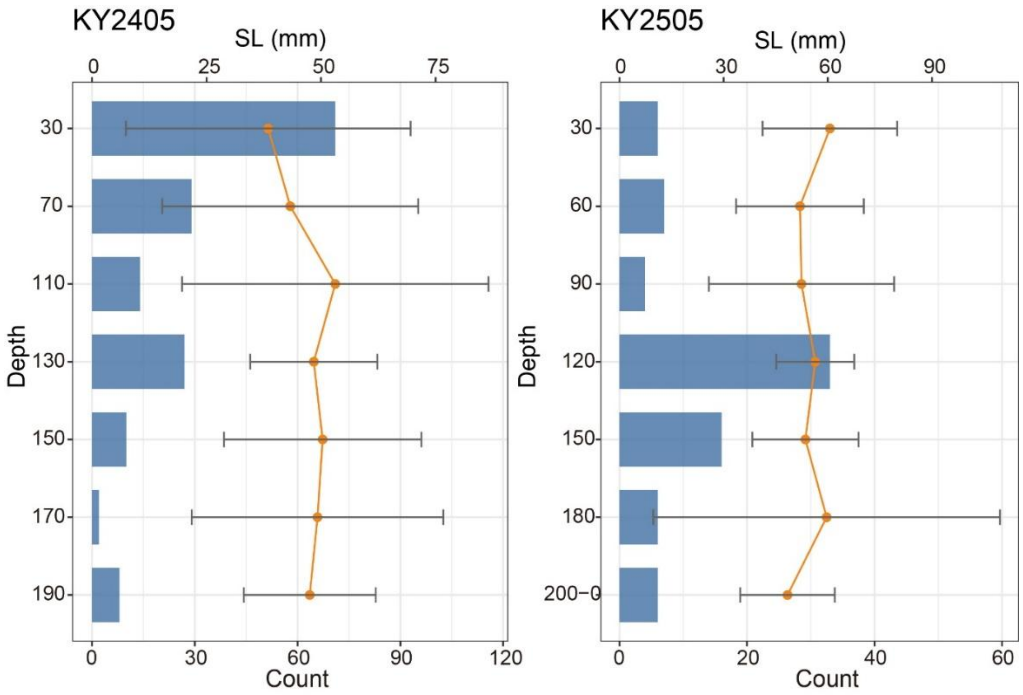

Fig. 18. Abundance and size composition of *Katsuwonus pelamis* collected in each depth-stratified midwater trawl tow. Bars indicate the number of individuals collected, while the line and error bars represent the mean fork length and standard deviation, respectively.

Other biological samples

Both surveys of the NORPAC net, the VMPS and Bongo net with 0.1mm mesh were conducted with 16 tows at all stations during this cruise. These zooplankton samples will be used to analyse the feeding environment of tuna larvae, as well as the relationship between oceanographic conditions and horizontal and the vertical distribution of zooplankton.

A large amount of biological samples except for tuna fishes were obtained by the midwater trawl surveys, for example, fish, squid, gelatinous, crustacean etc. (**Table 3, Fig. 17b**). The biomass varied depending on the location and water depth (**Table 3**). Species identification of the collected biological samples is currently in progress. In combination with the samples collected during the KY2024 cruise, these data will be used to characterize the biological community structure of this region.

Table 3 Wet weight (g) of all biological samples each station and depth collected by midwater trawl surveys

Depth	St.17	St.13	St.09	St.08	St.05	St.02
30m	15,300	12,450	19,400	1,294	12,050	228
60m	15,500	16,800	26,000	3,376	2,050	738
90m	36,900	10,850	26,400	8,872	4,300	882
120m	13,300	12,900	29,050	15,550	9,400	5,170
150m	38,250	13,900	19,900	17,150	5,750	1,890
180m	13,300	15,000	28,090	7,070	2,750	1,608
200-0m	16,700	14,800	27,000	8,604	2,250	995

Future perspective

During the KY2505 cruise, surveys were conducted to investigate the distribution of tropical tuna larvae and juveniles and their associated oceanographic environment. The survey area covered east–west transects centered on 180° longitude from the equator to 5°N (Leg 1) and a north–south transect along 150°E (Leg 2). This cruise yielded not only a large number of valuable biological samples but also important oceanographic and acoustic data that will contribute to a better understanding of the early life history of tropical tunas. Future work will involve integrated analyses of these data together with those collected during the KY2405 cruise, with a particular focus on the early life ecology of tropical tunas and their relationships with oceanographic conditions.

With the completion of the KY2405 and KY2505 cruises, two comprehensive surveys have been conducted in the study area, providing a robust scientific foundation for understanding the distribution and habitat characteristics of tropical tuna larvae and juveniles. Based on the findings from these cruises, the survey area will be shifted eastward in 2026. Specifically, a north–south survey transect has been established along 165°W. This region has received relatively little scientific survey effort in recent years. Therefore, the planned surveys in this region are expected to provide new insights into the ecology and distribution of tropical tunas, including their responses to recent oceanographic and climatic variability.

Acknowledgements

We expressed our acknowledgements to the Fisheries Agency of Japan to enable us and allow to conduct surveys by the R/V Kaiyo-Maru of Fisheries Agency.

References

Kodama, T., Shimizu, Y., Ichikawa, T., Hiroe, Y., Kusaka, A., Morita, H., Shimizu, M. & Hidaka, K. (2014). Seasonal and spatial contrast in the surface layer nutrient content around the Kuroshio along 138 °E, observed between 2002 and 2013. Journal of Oceanography, 70(6), 489–503. https://doi.org/10.1007/s10872-014-0245-5

Oozeki, Y., Hu, F. Tomatsu, C., Kubota, H. (2012) Development of a new multiple sampling trawl with

autonomous opening/closing net control system for sampling juvenile pelagic fish. Deep-Sea Research Part I-Oceanographic Research Papers 61, 100–108

Suzuki, R., & Ishimaru, T. (1990). An improved method for the determination of phytoplankton chlorophyll using N,N-dimethylformamide. Journal of the Oceanographical Society of Japan, 46(4), 190–194. https://doi.org/10.1007/BF02125580

Tawa, A., Ishihara, T., Matsubara, N., Hasegawa, T., Yamaguchi, T., Nagatomo, Y., Okazaki, M., Kusaka, A, Hidaka, K., Kiyofuji, H., Allain, V., Nicol, S., Hamer, P., Pilling, G. (2024) Pacific Tuna and Ecosystem Research Cruise Project. WCPFC-SC20-2024/EB-IP-11

Tawa, A., Ishihara, T., Matsubara, N., Hasegawa, T., Yamaguchi, T., Nagatomo, Y., Okazaki, M., Kusaka, A, Hidaka, K., Kiyofuji, H. Allain, V., Vourey, E., Barbin L., Magnier P., Nicol, S., Hamer, P., Pilling, G. (2025) Preliminary report of “Pacific Tuna and Ecosystem Research Cruise Project” in 2024. WCPFC-SC21-2025/EB-IP-16

Welschmeyer, N. A. (1994). Fluorometric analysis of chlorophyll a in the presence of chlorophyll b and phaeopigments. Limnology & Oceanography, 39(8), 1985–1992. https://doi.org/10.4319/lo.1994.39.8.198